AIMS Mathematics, 8(11): 25754–25771.
DOI: 10.3934/math.20231314
Received: 13 May 2023
Revised: 11 August 2023
Accepted: 21 August 2023
Published: 07 September 2023

http://www.aimspress.com/journal/Math

Research article

The mR scheme to the shallow water equation with horizontal density gradients in one and two dimensions

Kamel Mohamed[1,2,*], **H. S. Alayachi**[1] **and Mahmoud A. E. Abdelrahman**[1,3]

[1] Department of Mathematics, College of Science, Taibah University, Al-Madinah Al-Munawarah, Saudi Arabia

[2] Department of Mathematics, Faculty of Science, New valley University, New Valley, Egypt

[3] Department of Mathematics, Faculty of Science, Mansoura University, 35516 Mansoura, Egypt

* **Correspondence:** Email: mahmoud.abdelrahman@mans.edu.eg.

Abstract: In this work, we consider the model of shallow water equation with horizontal density gradients. We develop the modified Rusanov (mR) scheme to solve this model in one and two dimensions. Predictor and corrector are the two stages of the suggested scheme. The predictor stage is dependent on a local parameter ($\alpha^n_{i+\frac{1}{2}}$) that allows for diffusion control. The balance conservation equation is recovered in the corrector stage. The proposed approach is well-balanced, conservative, and straightforward. Several 1D and 2D test cases are produced after presenting the shallow water model and the numerical technique. In the 1D case, we compared the proposed scheme with the Rusanov scheme, mR with constant α and analytical solutions. The numerical simulation demonstrates the mR's great resolution and attests to its capacity to produce accurate simulations of the shallow water equation with horizontal density gradients. Our results demonstrate that the mR technique is a highly effective instrument for solving a variety of equations in applied science and developed physics.

Keywords: shallow water equation; modified Rusanov scheme; balance laws; source terms
Mathematics Subject Classification: 35L60, 35L67, 76M12, 86A05

1. Introduction

Recently, geophysical fluid dynamics modeling has grown in prominence due to the importance of forecasting and understanding the time development of a wide range of atmospheric and oceanic flows. The characteristics of the flows and the corresponding scales are used to construct models for simulating geophysical flows. A significant horizontal length scale in proportion to depth distinguishes several geophysical and atmospheric processes. That is, they are shallow, and shallow water equations

are suited for explaining their time evolution in those conditions [1]. The one-dimensional shallow water model in Eulerian coordinates is considered [2, 3].

One way to depict fluid flow is as a multi-layered flow where one layer flows over another to generate a new layer. The shallow water is a narrow layer of constant density fluid in hydrostatic equilibrium, bounded from below by a rigid surface and from above by a free surface. The shallow water model is one of the most vital models of the hyperbolic systems. In applied science and new physics, nonlinear hyperbolic systems of conservation laws are crucial for creating mathematical representations of a variety of natural processes [4–8]. It is the most fundamental layer example of an incompressible fluid moving across a free surface [9]. Utilizing this approach, channels, hydraulic jumps, tsunamis and reservoirs may all be simulated. Because the topography may be irregular and the geometry may be complicated, replicating these natural flow problems is difficult. Some bottom topographies need moving meshes in Eulerian coordinates that are stationary meshes in mass Lagrangian coordinates [2].

Various mathematical methods for finding analytical and numerical solutions to nonlinear partial differential equations (NPDEs) have been developed over the years [10–15]. In the ongoing work, we take into account a system of flows for shallow water where horizontal density fluctuations are considered. The Euler equations are vertically averaged to produce this model. We develop the mR scheme to solve the shallow water flows via horizontal density fluctuations. This approach has predictor and corrector stages. The Riemann invariants and limiters principles serve as the foundation for the control parameter for numerical diffusion through the predictor stage. The balance conservation equation is recovered in the corrector stage, see [16–21]. In most common schemes, the numerical flux was estimated using the Riemann solution. In contrast to earlier schemes, the intriguing property of the modified Rusanov (mR) scheme is to evaluate the numerical flux in the absence of the Riemann solution [22]. As long as the prerequisite for the canonical Courant-Friedrichs-Lewy (CFL) is obeyed, this scheme is linearly stable.

The remainder of this article's framework is constructed as follows. Section 2 introduces the mathematical model for shallow water equation with horizontal density gradients. Section 3 provides the 1D mR method to solve the proposed model. Section 4 shows various 1D test cases for investigating the development mechanisms of constructed waves. Section 5 depicts the 2D shallow water with horizontal density gradients. Section 6 offers various numerical test cases to check the accuracy and performance of the proposed scheme in 2D. Conclusions and observations about the current results are presented in Section 7.

2. Mathematical model

We consider the shallow water model with influences of horizontal density gradients, which given as follows [1]:

$$\begin{aligned} \frac{\partial(\rho h)}{\partial t} + \frac{\partial(\rho hu)}{\partial x} &= 0, \\ \frac{\partial(\rho hu)}{\partial t} + \frac{\partial\left(\rho hu^2 + \frac{1}{2}g\rho h^2\right)}{\partial x} &= -g\rho h\frac{\partial Z}{\partial x} \\ \frac{\partial(h)}{\partial t} + \frac{\partial(hu)}{\partial x} &= 0, \end{aligned} \tag{2.1}$$

h is the height of the water above the bottom, g is the gravity acceleration, u is the water velocity, Z is the function that describes the bottom topography and ρ is the vertical averaged density. The above system can write in the conservation form as the following

$$\frac{\partial W}{\partial t} + \frac{\partial F}{\partial x} = Q(W). \tag{2.2}$$

The vector-valued functions W; $F(W)$ and $Q(W)$ in R^3 are

$$W = \begin{pmatrix} \rho h \\ \rho hu \\ h \end{pmatrix}, \qquad F(W) = \begin{pmatrix} \rho hu \\ \rho hu^2 + \frac{1}{2} g\rho h^2 \\ hu \end{pmatrix}, \qquad \text{and} \qquad Q(W) = \begin{pmatrix} 0 \\ -g\rho h \frac{\partial Z}{\partial x} \\ 0 \end{pmatrix}. \tag{2.3}$$

It is clear that system of Eq (2.2) is strictly hyperbolic, and the associated eigenvalues are

$$\lambda_1 = u - \sqrt{gh}, \quad \lambda_2 = u \quad \text{and} \quad \lambda_3 = u + \sqrt{gh}. \tag{2.4}$$

3. Modified Rusanov scheme

The integration of the (2.2) on the domain $[x_{i-1/2}, x_{i+1/2}][t_n, t_{n+1}]$, which gives the finite volume scheme, which equivalent the corrector stage and we can be written as the following

$$W_i^{n+1} = W_i^n - \frac{\Delta t}{\Delta x}\left(F\left(W_{i+1/2}^n\right) - F\left(W_{i-1/2}^n\right)\right) + \Delta t {Q_i}^n, \tag{3.1}$$

W_i^n is the average value of the solution W over $[x_{i-1/2}, x_{i+1/2}]$ at time t_n *i.e.,*

$$W_i^n = \frac{1}{\Delta x}\int_{x_{i-1/2}}^{x_{i+1/2}} W(t_n, x)\, dx,$$

and $F(W_{i\pm1/2}^n)$ represents the numerical flux at the time t_n and place $x = x_{i\pm1/2}$. Generally, in the finite volume scheme (3.1), the Riemann solution at the cell interfaces $x_{i\pm1/2}$ is required for the building of the numerical fluxes $F(W_{i\pm1/2}^n)$. The objective is to create the intermediate states, which are denoted by $W_{i\pm1/2}^n$. To achieve this, we must integrate the Eq (2.2) through the interval $[t_n, t_n + \theta_{i+1/2}^n] \times [x^-, x^+]$. We achieve the intermediate state, which has the following written form:

$$\begin{aligned} &\int_{x^-}^{x^+} W(t_n + \theta_{i+1/2}^n, x)\, dx \\ = \;& \Delta x^- W_i^n + \Delta x^+ W_{i+1}^n - \theta_{i+1/2}^n\Big(F(W_{i+1}^n) - F(W_i^n)\Big) + \theta_{i+1/2}^n(\Delta x^- - \Delta x^+)Q_{i+\frac{1}{2}}^n, \end{aligned} \tag{3.2}$$

whereas, the distance measurements, Δx^- and Δx^+ can be stated as follows.

$$\Delta x^- = \left|x^- - x_{i+1/2}\right|, \qquad \Delta x^+ = \left|x^+ - x_{i+1/2}\right|.$$

$Q_{i+\frac{1}{2}}^n$ refers to an approximation of the source term $Q(W)$

$$Q_{i+\frac{1}{2}}^n = \frac{1}{\theta_{i+\frac{1}{2}}^n(\Delta x^- + \Delta x^+)}\int_{t_n}^{t_n+\theta_{i+\frac{1}{2}}^n}\int_{x^-}^{x^+} Q(W) dt\, dx. \tag{3.3}$$

When, we substitute x^- by x_i and x^+ by x_{i+1} in the Eq (3.2), we get the following equation.

$$W^n_{i+1/2} = \frac{1}{2}\left(W^n_i + W^n_{i+1}\right) - \frac{\theta^n_{i+1/2}}{\Delta x}\Big(F(W^n_{i+1}) - F(W^n_i)\Big) + \theta^n_{i+\frac{1}{2}} Q^n_{i+\frac{1}{2}}, \tag{3.4}$$

whereas $W^n_{i+1/2}$ is define as the following are additional alternatives for x^+ and x^-. According to the stability analysis in [16] for conservation laws, we selected the control parameter $\theta^n_{j+1/2}$ for completing our scheme, and we are able to pick the parameter $\theta^n_{j+1/2}$ as follows:

$$W^n_{i+1/2} = \frac{1}{\Delta x}\int_{x_i}^{x_{i+1}} W(x, t_n + \theta^n_{i+1/2})dx. \tag{3.5}$$

The Eq (3.2) shows that the

$$\theta^n_{i+1/2} = \alpha^n_{i+1/2}\bar{\theta}_{i+1/2}, \qquad \bar{\theta}_{i+1/2} = \frac{\Delta x}{2S^n_{i+1/2}}, \tag{3.6}$$

whereas

$$S^n_{i+1/2} = \max_{k=1,\ldots,K}(max(|\lambda^n_{k,i}|, |\lambda^n_{k,i+1}|)), \tag{3.7}$$

$$s^n_{i+1/2} = \min_{k=1,\ldots,K}(max(|\lambda^n_{k,i}|, |\lambda^n_{k,i+1}|)), \tag{3.8}$$

and the control parameter is $\alpha^n_{i+1/2}$. The kth eigenvalue of (2.2) is represented by $\lambda^n_{k,i}$ and k is the number of of eigenvalues of the system (2.2). As a result of this discussion, we can choose the control parameter in the following ways:

i) $\alpha^n_{i+1/2} = 1$, the mR scheme becomes the upwind scheme in the linear case with this decision [16].

ii) $\alpha^n_{i+1/2} = \frac{\Delta t}{\Delta x} S^n_{i+1/2}$, by making this decision, the suggested scheme return to the Lax-Wendroff scheme.

iii) $\alpha^n_{i+1/2} = \tilde{\alpha}^n_{i+1/2} = \frac{S^n_{i+1/2}}{s^n_{i+1/2}}$, with this decision, the scheme is transformed into a first-order scheme.

iv) All calculations in this paper were made using the following formula for

$$\alpha^n_{i+1/2} = (1 - \Phi(r_{i+1/2}))\frac{S^n_{i+1/2}}{s^n_{i+1/2}} + \frac{\Delta t}{\Delta x} S^n_{i+1/2}\Phi(r_{i+1/2}), \tag{3.9}$$

where $\Phi_{i+1/2} = \Phi\left(r_{i+1/2}\right)$ is a function that limits slope, with

$$r_{i+1/2} = \frac{W_{i+1-q} - W_{i-q}}{W_{i+1} - W_i}, \qquad q = \operatorname{sgn}\left[F'(X^{n+1}, W^n_{i+1/2})\right].$$

At last, we write the propose scheme for shallow water equation with horizontal density gradients as the following

$$\begin{cases} W^n_{i+1/2} = \frac{1}{2}\left(W^n_i + W^n_{i+1}\right) - \frac{\alpha^n_{i+1/2}}{2S^n_{i+1/2}}\Big(F(W^n_{i+1}) - F(W^n_i)\Big) + \frac{\alpha^n_{i+1/2}}{2S^n_{i+1/2}}\Delta x Q^n_{i+\frac{1}{2}}, \\ W^{n+1}_i = W^n_i - \frac{\Delta t}{\Delta x}\left(F\left(W^n_{i+1/2}\right) - F\left(W^n_{i-1/2}\right)\right) + \Delta t {Q_i}^n. \end{cases} \tag{3.10}$$

The proposed scheme is well-balanced in the sense of [23–25], if the source term Q^n_i in the corrector stage is approximated in such a way that the still-water balance (C-property) [26] is obeyed, if the condition

$$u = 0, \qquad h + Z = constant, \qquad \text{and} \qquad \rho = constant \tag{3.11}$$

is satisfied the steady state solutions, then, we said the numerical scheme for the shallow water equation with horizontal density gradients satisfies the C-property.

Proof of the exact C-property. In (2.1) and (2.2), we assume that $u = 0$, which represents a stationary flow in rest. Then Eq (2.1) can be written as follows

$$\partial_t \begin{pmatrix} \rho h \\ 0 \\ h \end{pmatrix} + \partial_x \begin{pmatrix} 0 \\ \frac{1}{2}\rho g h^2 \\ 0 \end{pmatrix} = \begin{pmatrix} 0 \\ -g\rho h \partial_x Z \\ 0 \end{pmatrix}. \tag{3.12}$$

We applied the predictor stage in (3.10) for the system (3.12), we have

$$W^n_{i+\frac{1}{2}} = \begin{pmatrix} \frac{1}{2}((\rho h)^n_i + (\rho h)^n_{i+1}) \\ -\frac{\rho^n_i \alpha^n_{i+\frac{1}{2}}}{4S^n_{i+\frac{1}{2}}} g(h^n_{i+1} + h^n_i)[h^n_{i+1} - h^n_i + Z_{i+1} - Z_i] \\ \frac{1}{2}((h^n_i + h^n_{i+1}) \end{pmatrix} = \begin{pmatrix} \frac{1}{2}((\rho h)^n_i + (\rho h)^n_{i+1}) \\ 0 \\ \frac{1}{2}(h^n_i + h^n_{i+1}) \end{pmatrix}. \tag{3.13}$$

During the corrector stage, the solution is updated as

$$\begin{pmatrix} (\rho h)^{n+1}_i \\ (\rho h u)^{n+1}_i \\ h^{n+1}_i \end{pmatrix} = \begin{pmatrix} (\rho h)^n_i \\ (\rho h u)^n_i \\ h^n_i \end{pmatrix} - \frac{rg\rho^n}{2} \begin{pmatrix} 0 \\ (h^n_{i+\frac{1}{2}})^2 - (h^n_{i-\frac{1}{2}})^2 \\ 0 \end{pmatrix} + \begin{pmatrix} 0 \\ \Delta t_n Q^n_i \\ 0 \end{pmatrix}. \tag{3.14}$$

To obtain a stationary solution $W^{n+1}_i = W^n_i$, the sum of the discretized flux gradients and source terms in Eq (3.12) must be equal to zero.

$$\frac{r\rho^n}{2} g((h^n_{i+\frac{1}{2}})^2 - (h^n_{i-\frac{1}{2}})^2) = -(gh\rho\partial_x Z)^n_i. \tag{3.15}$$

Then, the previous expression (3.15), which is equivalent to

$$(gh\rho\partial_x Z)^n_i = -\frac{g}{8\Delta x}((\rho h)^n_{i+1} + 2(\rho h)^n_i + (\rho h)^n_{n-1})(Z_{i+1} - Z_{i-1}). \tag{3.16}$$

Therefore, if the source term in the corrector stage of Eq (3.16) is discretized as follows

$$\begin{pmatrix} 0 \\ -\frac{g}{8\Delta x}((\rho h)^n_{i+1} + 2(\rho h)^n_i + (\rho h)^n_{n-1})(Z_{i+1} - Z_{i-1}) \\ 0. \end{pmatrix} \tag{3.17}$$

the proposed scheme satisfied the C-property.

4. Numerical results

We present several test cases for numerical simulation of the shallow water equation with horizontal density gradients. We selected the stability condition [16] in the manner described below in order to demonstrate the effectiveness and accuracy of the suggested finite volume scheme

$$\Delta t = CFL \frac{\Delta x}{\max_i(\left|\alpha^n_{i+\frac{1}{2}} S^n_{i+\frac{1}{2}}\right|)}, \tag{4.1}$$

where the chosen constant CFL equals 0.5.

4.1. *Test* 1

With the following initial conditions [1], this case's solution includes a rarefaction wave; contact discontinuity; shock wave:

$$(h,u,\rho) = \begin{cases} (13.41, 5, 0.1) & \text{if} \quad x \leq 0, \\ (3, 5, 2) & \text{if} \quad x > 0. \end{cases} \tag{4.2}$$

This test case is simulated using modified Rusanov and classical Rusanov, when compared to the reference solution produced by applying the classical Rusanov technique with a smaller mesh size of 30000 uniform cells over the range $[-10, 10]$ and time t=1 s with gravity ($g = 1$). Figures 1–3 show the results of water height, velocity, density, quantity of movement, pressure and parameter of control. For the another the domain $[0, 12]$ and gravity 9.81, we simulate this test case with a more refined mesh of 20000 uniform cells. In this case, Figures 4–6 show the results.

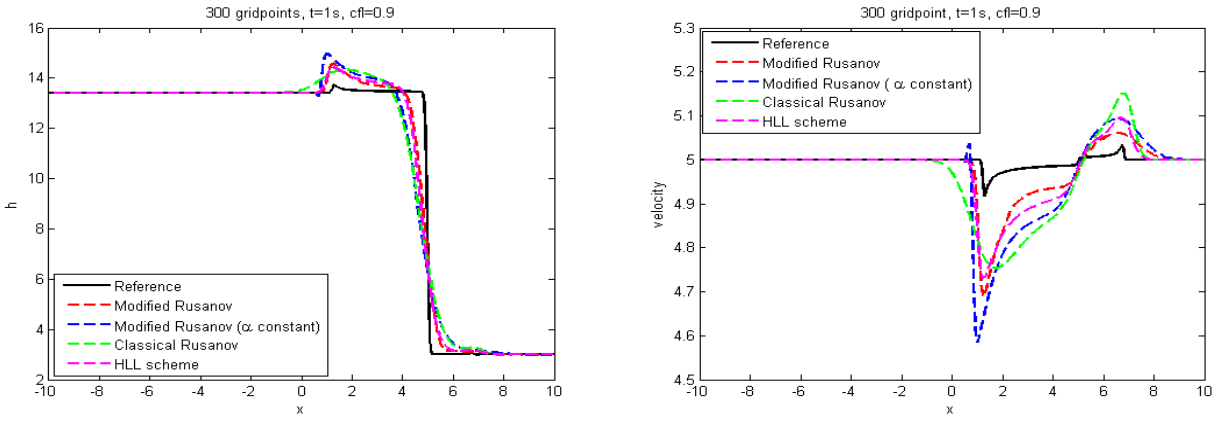

Figure 1. Water height and speed at t=1 s.

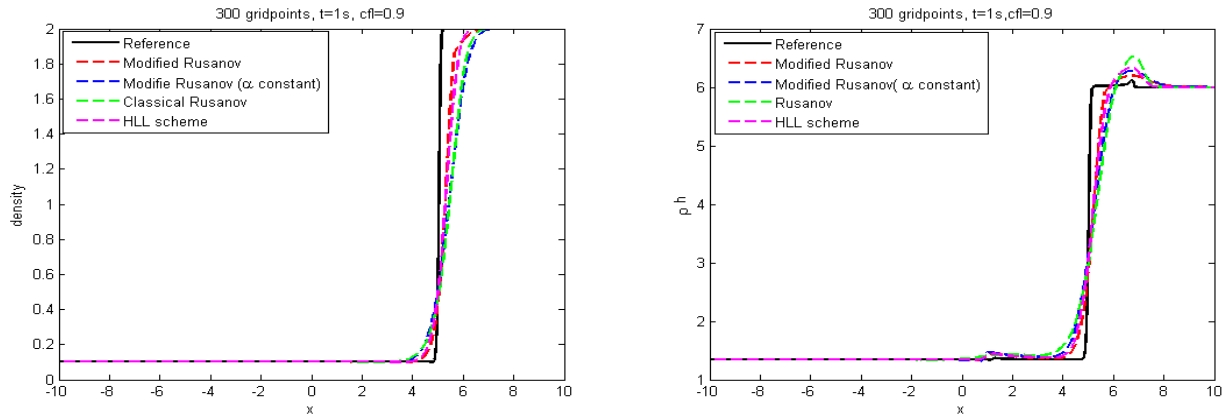

Figure 2. Water density and quantity of movement at t=1 s.

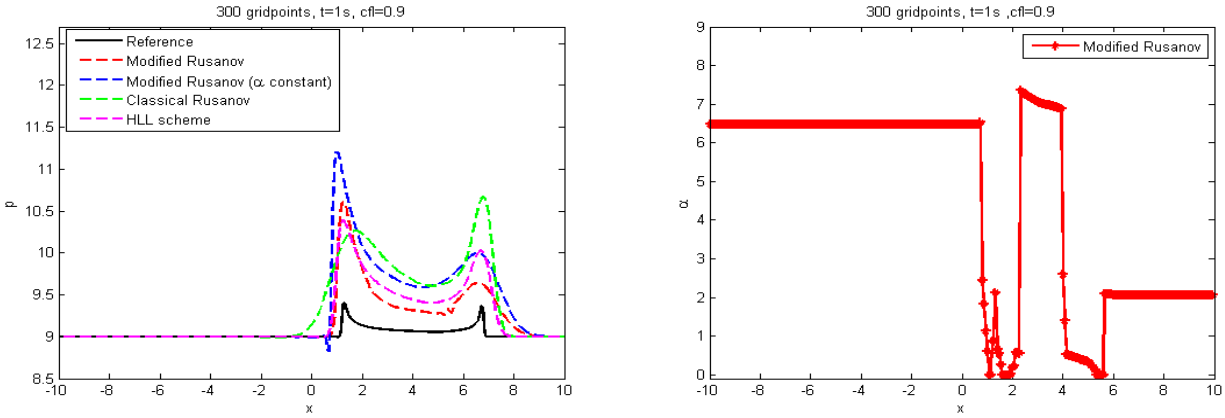

Figure 3. Pressure and $\alpha^n_{i+\frac{1}{2}}$ at t=1 s.

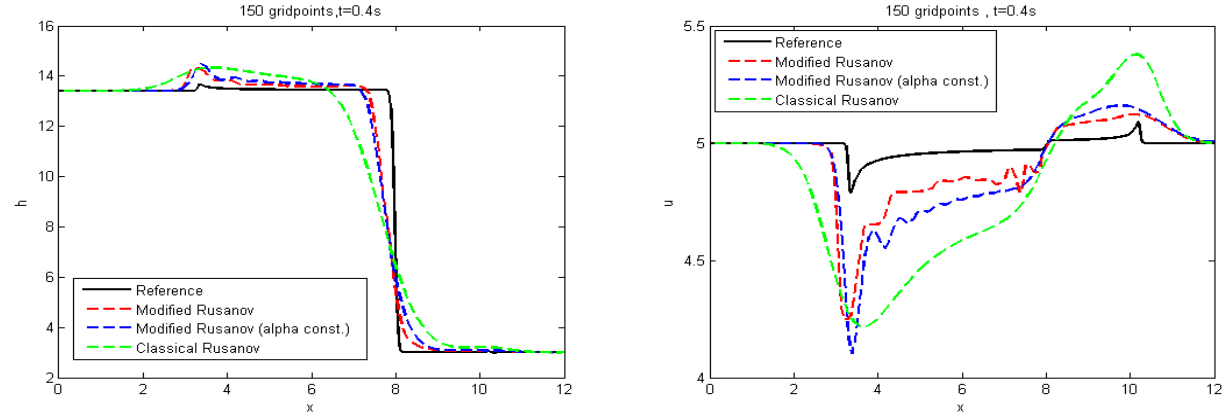

Figure 4. Water height and speed at t=0.5 s.

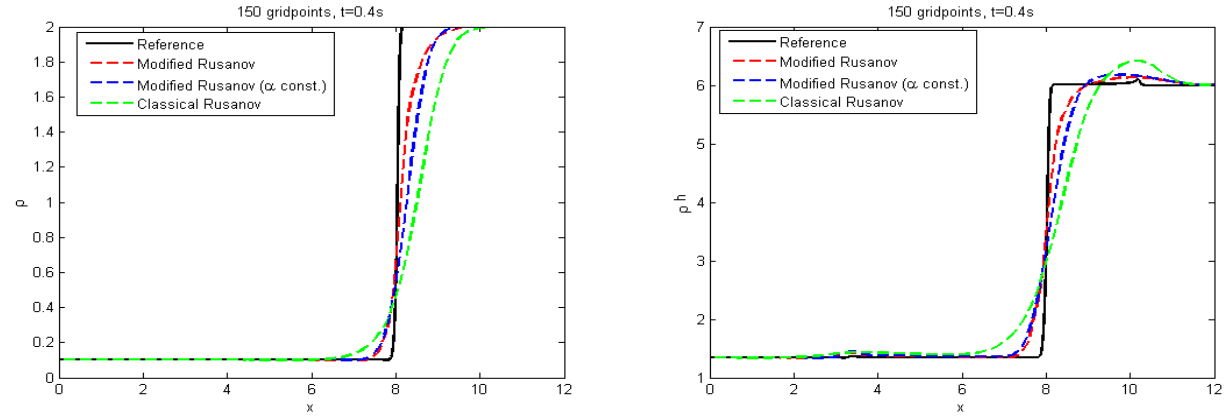

Figure 5. Water density and quantity of movement at t=0.4 s.

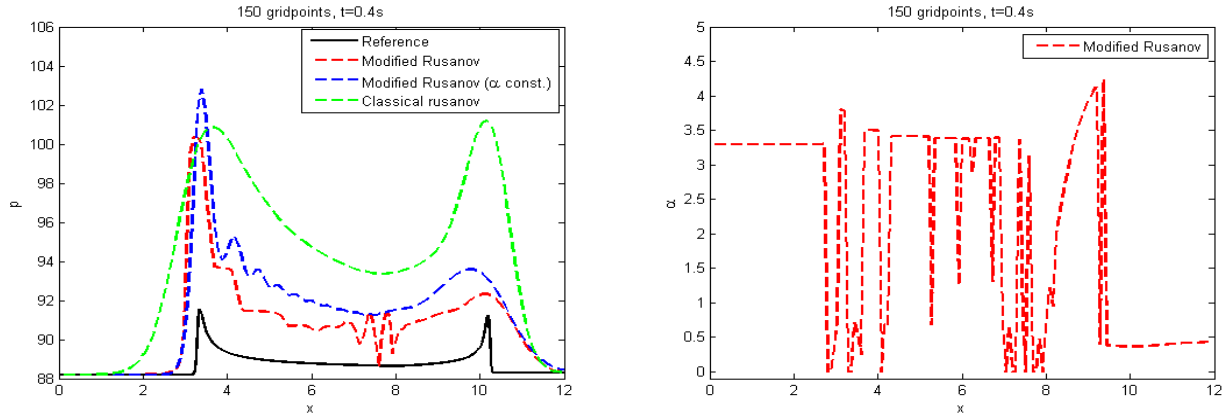

Figure 6. Pressure and $\alpha^n_{i+\frac{1}{2}}$ at t=0.4 s.

4.2. Test 2

According to the initial conditions listed in [4], this example has been suggested:

$$(h, u, \rho) = \begin{cases} (33.0416, 5.9484, 0.1) & \text{if} \quad x \leq 0, \\ (4, 6.5, 4) & \text{if} \quad x > 0.5. \end{cases} \tag{4.3}$$

The mesh has 300 cells and the domain of computation is $[-10, 10]$ with a final time of t=0.5 s, by applying the mR technique and the classical Rusanov method. Figure 7 displays the numerical results for the water height and velocity, which are contrasted with the reference solution that was produced utilizing the classical Rusanov method and a finer mesh made up of 30000 uniform cells. We find that the results from the modified Rusanov scheme are more precise than those from the classical and modified Rusanov schemes with alpha constant ($\alpha^n_{i+\frac{1}{2}} = 1.4$). Figure 8 shows the density and quantity of movement. Figure 9 shows the pressure and $\alpha^n_{i+\frac{1}{2}}$.

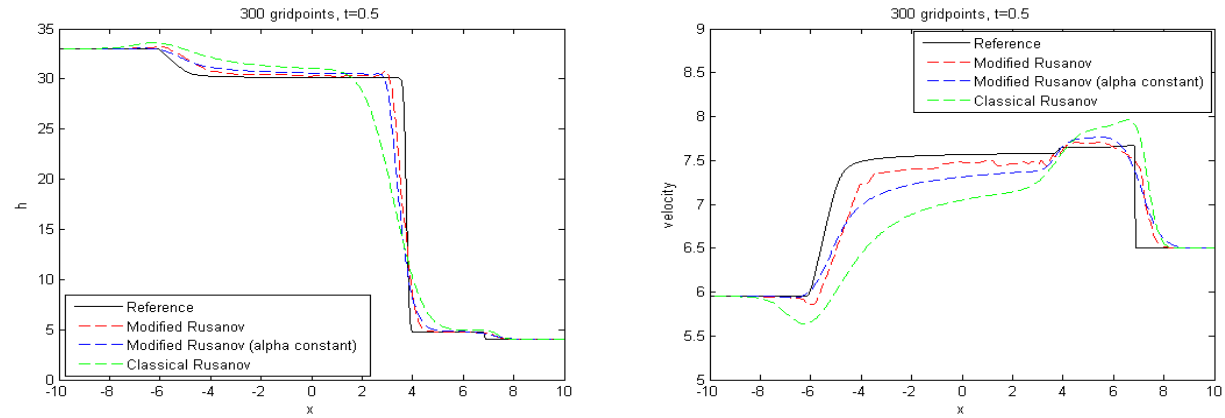

Figure 7. Water height and velocity at t= 0.5 s.

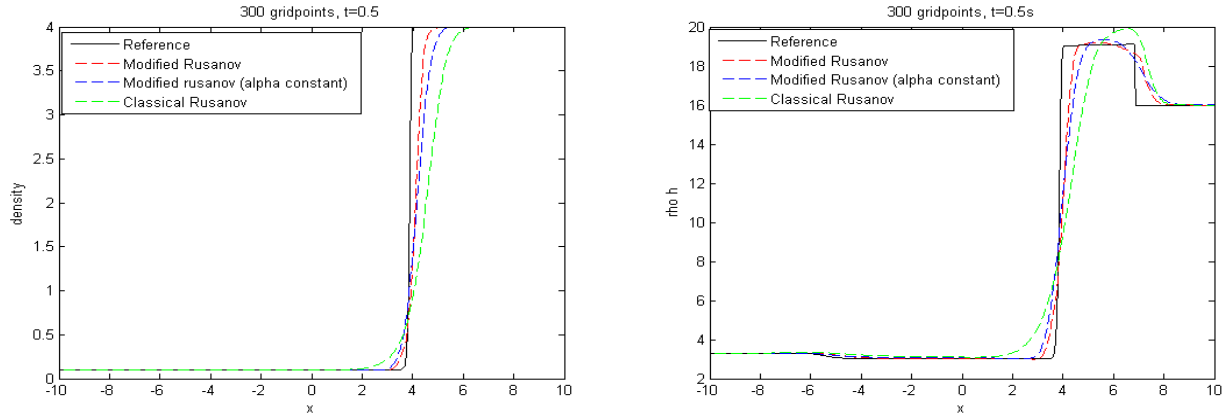

Figure 8. Water density and quantity of movement at t=0.5 s.

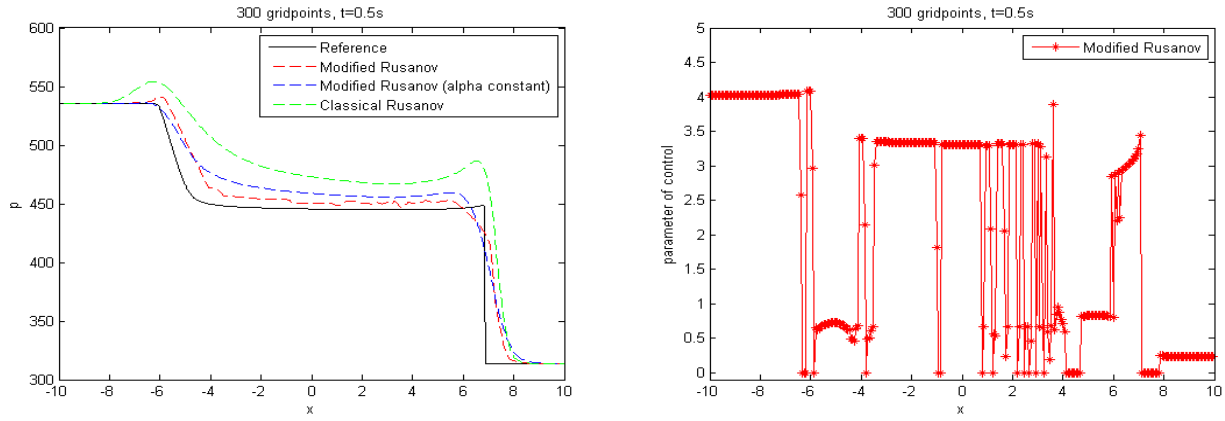

Figure 9. Pressure and $\alpha^n_{i+\frac{1}{2}}$ at t=0.5 s.

4.3. Test 3 *non homogeneous*

We consider the same case in the first example with source term as follows

$$(h,u,\rho,Z) = \begin{cases} (13.41,5,0.1,0) & \text{if} \quad x \leq 0, \\ (3,5,2,1) & \text{if} \quad x > 0. \end{cases} \tag{4.4}$$

This test case is simulated using classical Rusanov and modified Rusanov, when compared to the reference solution produced by the classical Rusanov method using a smaller mesh size of 20000 cells over the interval $[0,12]$ and time t=0.4 s, with gravity ($g = 9.81$). Figures 10–12 show the results of water height, velocity, density, quantity of movement, pressure and parameter of control.

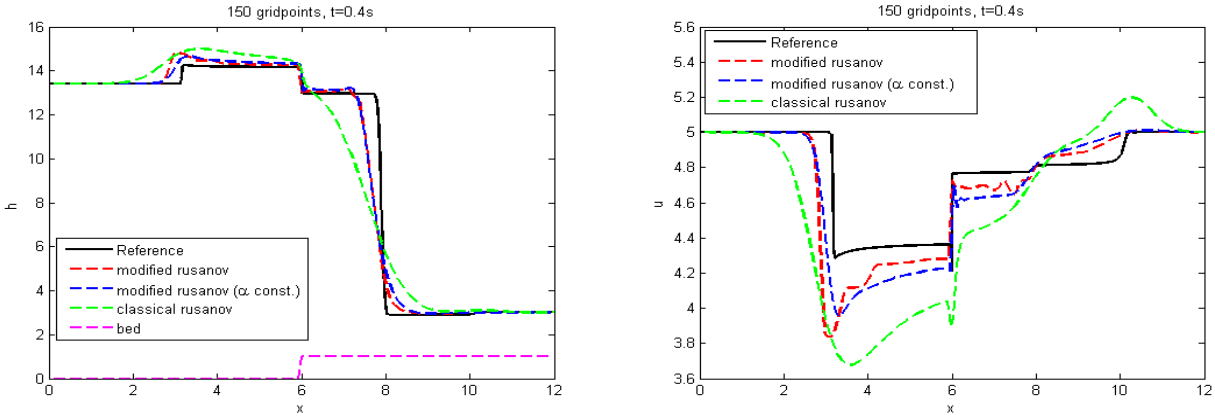

Figure 10. Water height and speed at t=0.4 s.

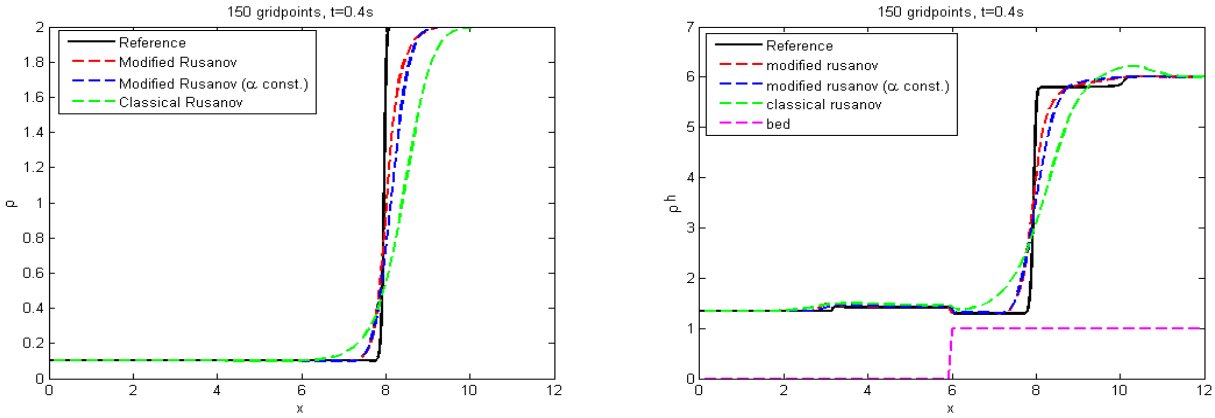

Figure 11. Water density and quantity of movement at t=0.4 s.

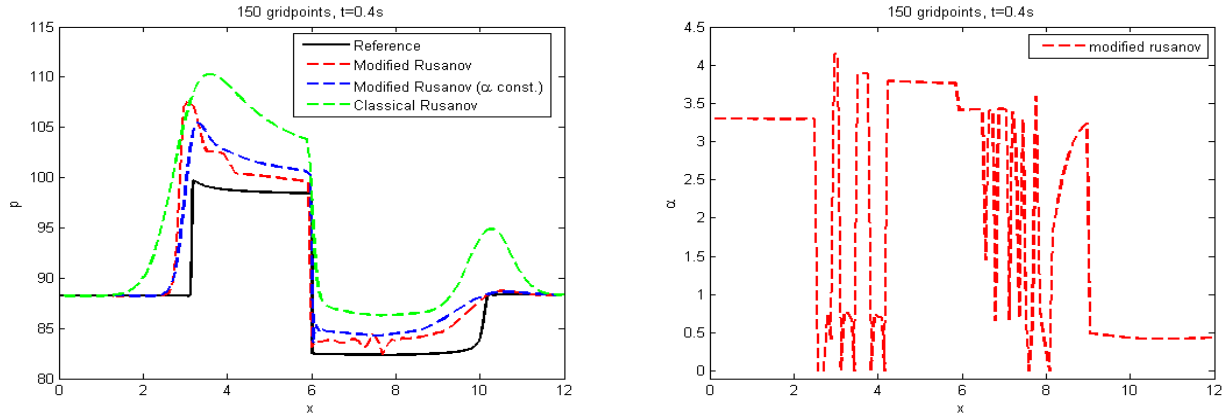

Figure 12. Pressure and $\alpha^n_{i+\frac{1}{2}}$ at t=0.4 s.

4.4. *Test* 4 *non homogeneous*

We consider the same case in the first example with source term and we can write it as follows

$$(h,u,\rho,Z) = \begin{cases} (13.41,5,0.1,0) & \text{if} \quad x \leq 0, \\ (3,5,2,1) & \text{if} \quad x > 0. \end{cases} \tag{4.5}$$

Modified Rusanov and classical Rusanov are used to simulate this test case, in comparison to the reference solution produced by the classical Rusanov method using a smaller grid of 20000 uniform cells over the interval [0, 12] and time t=0.4 s, with gravity ($g = 9.81$). Figures 13–15 show the results height, velocity, density, quantity of movement, pressure and parameter of control. Also, Figure 16 shows the effect of parameter of control ($\alpha = 1, 1, 5, 2, 2.5$) on the diffusion of density and quantity of movement.

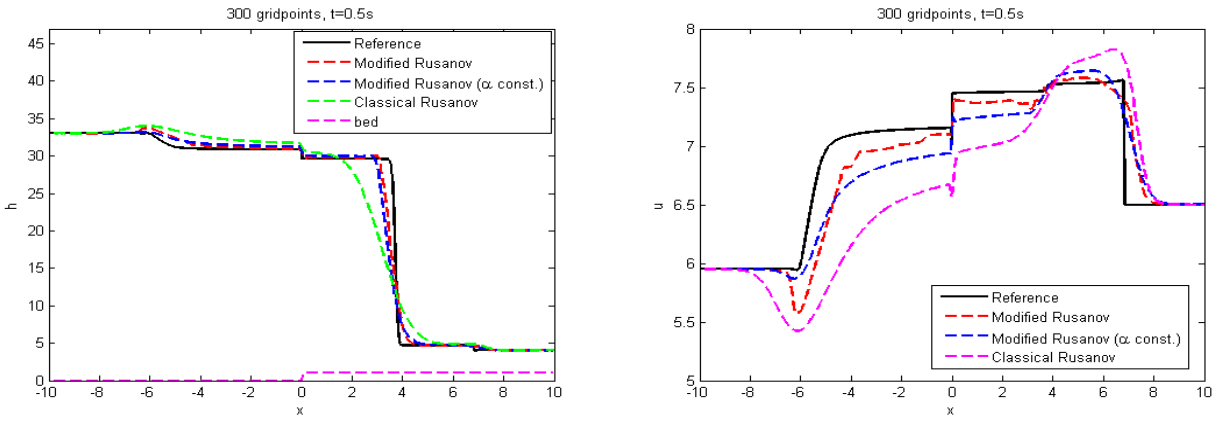

Figure 13. Water height and speed at t=0.5 s.

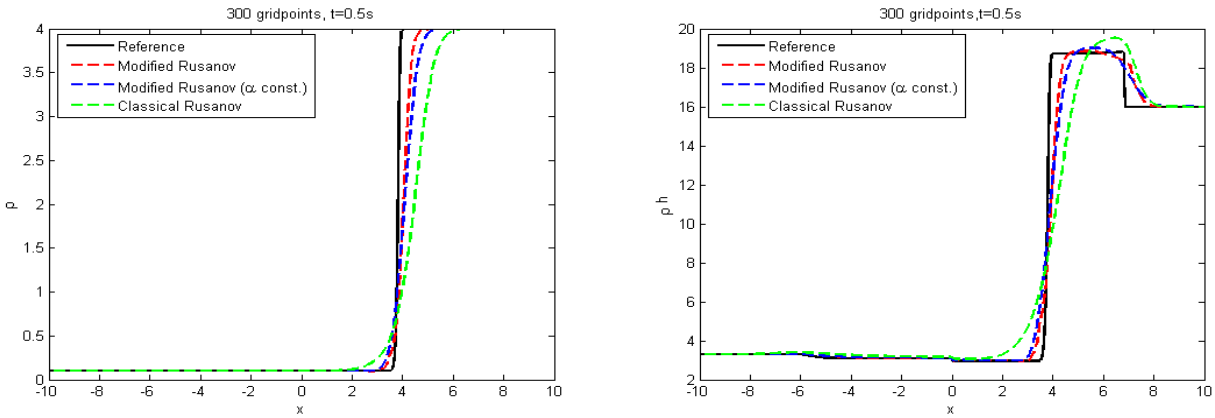

Figure 14. Water density and quantity of movement at t=0.5 s.

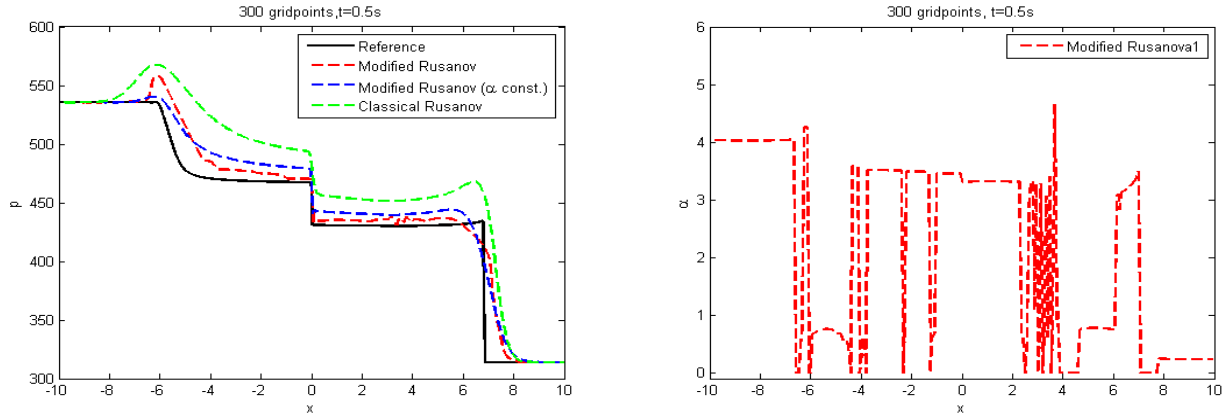

Figure 15. Pressure (left) and $\alpha^n_{i+\frac{1}{2}}$ (right) at t=0.5 s.

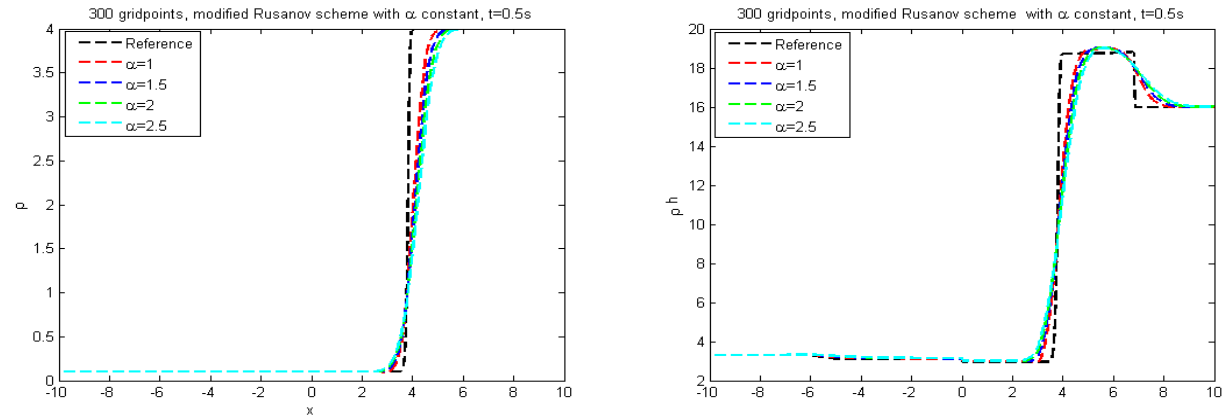

Figure 16. Water density and quantity of movement at t=0.5 s.

5. Two-dimensional shallow water with horizontal density gradients

The shallow water with horizontal density gradients can be expressed as follows in two dimensions:

$$\frac{\partial W}{\partial t} + \frac{\partial \mathbf{F}(\mathbf{W})}{\partial x} + \frac{\partial \mathbf{G}(\mathbf{W})}{\partial y} = \mathbf{Q}(\mathbf{W}), \tag{5.1}$$

with

$$\mathbf{W} = \begin{pmatrix} \rho h \\ \rho hu \\ \rho hv \\ h \end{pmatrix}, \qquad \mathbf{F}(\mathbf{W}) = \begin{pmatrix} \rho hu \\ \rho hu^2 + \frac{1}{2} g \rho h^2 \\ \rho huv \\ hu \end{pmatrix}, \tag{5.2}$$

and

$$\mathbf{G}(\mathbf{W}) = \begin{pmatrix} \rho hv \\ \rho huv \\ \rho hv^2 + \frac{1}{2}g\rho h^2 \\ hv \end{pmatrix}, \qquad \mathbf{Q}(\mathbf{W}) = \begin{pmatrix} 0 \\ -g\rho h\frac{\partial Z}{\partial x} \\ -g\rho h\frac{\partial Z}{\partial y} \\ 0 \end{pmatrix}. \tag{5.3}$$

where ρ, h, u, v are the density, water height and velocity respectively

5.1. Two-dimensional problems with modified Rusanov scheme

In order to deducing the modified Rusnov scheme in two dimension, we integrate the Eq (5.1) on a generic control volume c_i as shown in Figure 17, which are produced when the domain is divided into several control volumes, presents

$$W_i^{n+1} = W_i^n - \frac{\Delta t}{A_i}\sum_{j\in K(i)}\int_{\gamma_{ij}} \mathcal{F}(W, \vec{n}_{ij})d\sigma + \frac{\Delta t_n}{A_i}\int_{c_i} Q(x, y, W)\, dx\, dy, \tag{5.4}$$

where A_i refers to the cell's area c_i, $K(i)$ is the index set of adjacent triangles that share an edge with the cell c_i, $\vec{n}_{ij}$ denotes the unit outward normal vector to the surface that surround the control volume, $\int_{\gamma_{ij}} \mathcal{F}(W, \vec{n}_{ij})d\sigma = \phi(W_i^n, W_j^n, \vec{n}_{ij})mes(\gamma_{ij})$ is the numerical flux, $mes(\gamma_{ij})$ is the interface between cells c_i and c_j, with W_i^n and W_j^n are the left and right values of W at cell c_i and c_j.

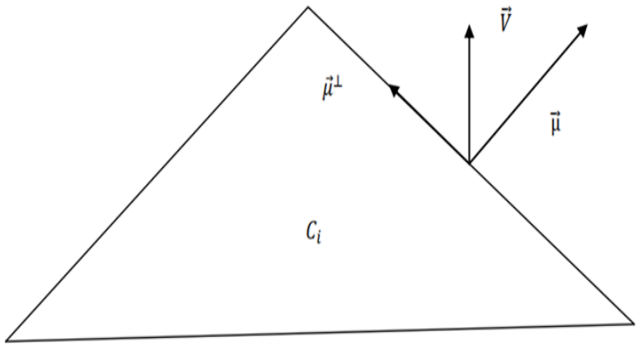

Figure 17. The control volume.

It is possible to express the modified Rusanov scheme as

$$\begin{cases} W_{ij}^n = \dfrac{1}{2}(W_i^n + W_{i+1}^n) - \dfrac{\alpha_{ij}^n}{2S_{ij}^n}\left[\mathcal{F}(W_j^n) - \mathcal{F}(W_i^n)\right]\cdot\vec{n}_{ij} + \dfrac{\alpha_{ij}^n}{2S_{ij}^n}Q_{ij}^n, \\ W_i^{n+1} = W_i^n - \dfrac{\Delta t}{A_i}\displaystyle\sum_{j\in K(i)}\phi(W_i^n, W_j^n, \vec{n}_{ij})mes(\gamma_{ij}) + \Delta t_n Q_i^n, \end{cases} \tag{5.5}$$

where S_{ij}^n is the local Rusanov speed represented by

$$S_{ij}^n = \max_p((|\lambda_{p,i}^n|, |\lambda_{p,j}^n|)),$$

and the local control parameter α_{ij}^n is chosen to meet the stability condition; for more information, see [16]. The eigenvalues of the Jacobien matrix (5.1) are$\lambda_{p,i}^n$ and $\lambda_{p,j}^n$.

5.2. Calculation of W_{ij}^n

Here, we aim to rewrite the numerical flux to resemble the 1D situation. To achieve this, we write $\phi(W_i^n, W_j^n, \vec{n}_{ij}) = \mathcal{F}(W_{ij}^n, \vec{n}_{ij})$, W_{ij}^n is determined at the predictor stage. To determine the W_{ij}^n, we project the system (5.1) on the local cell's outward normal μ and tangential $\mu^\perp$ as shown in Figure 17. Then, we have

$$\begin{cases} \dfrac{\partial \rho h}{\partial t} + \dfrac{\partial \rho h U}{\partial \mu} = 0, \\ \dfrac{\partial \rho h U}{\partial t} + \dfrac{\partial (\rho h U^2 + p)}{\partial \mu} + g\rho h \dfrac{dZ}{d\mu} = 0, \\ \dfrac{\partial \rho h V}{\partial t} + \dfrac{\partial \rho h U V}{\partial \mu} = 0, \\ \dfrac{\partial h}{\partial t} + \dfrac{\partial h U}{\partial \mu} = 0, \end{cases} \tag{5.6}$$

where $U = \vec{V} \cdot \eta = un_x + vn_y$ represent the normal speed and $V = \vec{V} \cdot \mu^\perp = -un_y + vn_x$ represents the tangential velocity. The predictor phase (5.5) expressed as

$$\begin{cases} (\rho h)_{ij} = M_{ij}(\rho h) - \dfrac{\alpha_{ij}^n}{2S_{ij}^n} \Delta_{ij}(\rho h U), \\ (\rho h U)_{ij} = M_{ij}(\rho h U) - \dfrac{\alpha_{ij}^n}{2S_{ij}^n} \Delta_{ij}(\rho h U^2 + p) - \dfrac{\alpha_{ij}^n}{2S_{ij}^n} g\tilde{\rho h}_{ij} \Delta_{ij}(Z), \\ (\rho h V)_{ij} = M_{ij}(\rho h V) - \dfrac{\alpha_{ij}^n}{2S_{ij}^n} \Delta_{ij}(\rho h U V), \\ (h)_{ij} = M_{ij}(h) - \dfrac{\alpha_{ij}^n}{2S_{ij}^n} \Delta_{ij}(h U), \end{cases} \tag{5.7}$$

with $\Delta_{ij}(X) = X_j - X_i$ and $M_{ij}(X) = \frac{1}{2}(X_i + X_j)$. Where $\tilde{\rho h}_{ij}$ is the linear interpolation between $(\rho h)_i$ and $(\rho h)_j$ given by $\tilde{\rho h}_{ij} = \dfrac{A_i(\rho h)_i + A_j(\tilde{\rho h})_j}{A_i + A_j}$. The solution W_{ij}^n is recovered via the transformation

$$(hu)_{ij} = n_x(hU)_{ij} - n_y(hV)_{ij}$$

and

$$(hv)_{ij} = n_y(hU)_{ij} + n_x(hV)_{ij}.$$

6. Numerical results in two dimensions

To test the precision and effectiveness of the suggested scheme in 2D, we provide several test cases. Due to presented CFL condition [16], the theoretical maximum stable time step Δt is specified.

$$\Delta t \max_i \left(\frac{|\delta C_i|}{A_i} \right) \left[1 + \alpha \frac{M}{m} \right] \frac{M}{2} = Cr, \tag{6.1}$$

the constant Currant number Cr is chosen to be less than unity, in this case $Cr = 0.2$ in all simulations, and the time step Δt is changed using Eq (6.1), with $M = \underset{i,j}{max}(S^n_{ij})$, $m = \underset{i,j}{min}(s^n_{ij})$, where S^n_{ij} is the local Rusanov speed, A_i refers to the cell's area c_i, the control parameter for the suggested scheme is $\alpha^n_{ij} = 1.8$, and $|\delta C_i|$ denotes the perimeter of the cell C_i.

We consider the this test case with and without source term. The initial conditions are

$$(h, u, v, \rho, Z) = \begin{cases} (13.41, 5, 0, 0.1, 0) & \text{if} \quad x \leq 0, \\ (3, 5, 0, 2, 1) & \text{if} \quad x > 0. \end{cases} \tag{6.2}$$

At the end, we simulate this test case using the mR scheme on the domain $[0, 12] \times [0, 1]$ meshgrid 150×15 equivalent 1903 cells and final time $t = 0.4$. Figures 18–20 display water height, velocity and density with out and with source term.

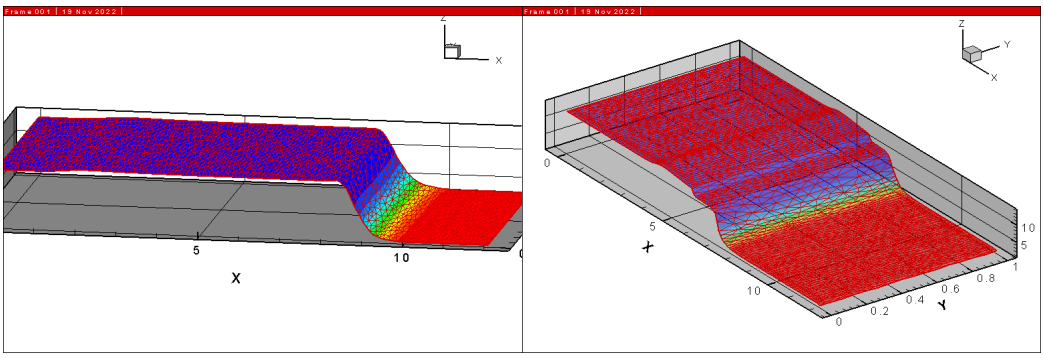

Figure 18. Water height without bed and water height with bed at t=0.4 s.

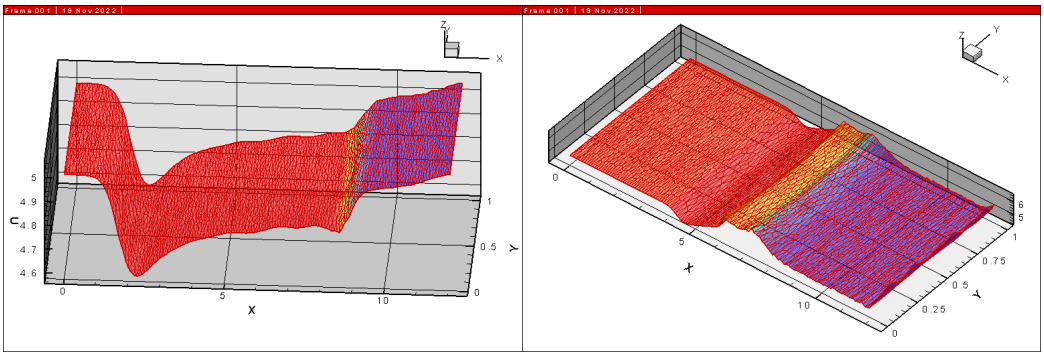

Figure 19. Velocity without bed and velocity with bed at t=0.4 s.

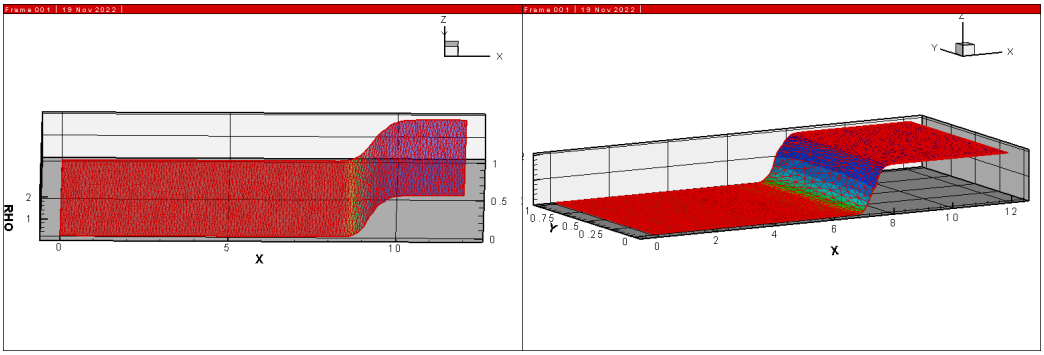

Figure 20. Density without bed and density with bed at t=0.4 s.

7. Conclusions

The mR scheme was proposed and applied to numerically simulate the shallow water equation with horizontal density gradients. This approach can properly represent discontinuance profiles and prevents numerical diffusion in the solution. In contrast to earlier schemes, the mR scheme has the intriguing ability to compute the numerical flow in the absence of the Riemann solution. This method, in fact, can be utilized as a box solver for a wide range of other conservation law models. Numerical results in one and two dimensions were introduced to depict the efficiency of the presented scheme. The Rusanov approach and analytical solutions were compared with the mR scheme. Several test cases were introduced in 1D and 2D. The numerical results display the high resolution of the proposed mR scheme and show that it can provide precise and effective simulations for the shallow water equation with horizontal density gradients.

Use of AI tools declaration

The authors declare they have not used Artificial Intelligence (AI) tools in the creation of this article.

Acknowledgments

The authors extend their appreciation to the Deputyship for Research & Innovation, Ministry of Education in Saudi Arabia for funding this research work through the project number 445-9-164.

Conflict of interest

The authors declare that they have no competing interests.

References

1. G. Hernandez-Duenas, A hybrid method to solve shallow water flows with horizontal density gradients, *J. Sci. Comput.*, **73** (2017), 753–782. https://doi.org/10.1007/s10915-017-0553-1

2. V. A. Dorodnitsyn, E. I. Kaptsov, Discrete shallow water equations preserving symmetries and conservation laws, *J. Math. Phys.*, **62** (2021), 083508. https://doi.org/10.1063/5.0031936

3. V. A. Dorodnitsyn, E. I. Kaptsov, Shallow water equations in Lagrangian coordinates: symmetries, conservation laws and its preservation in difference models, *Commun. Nonlinear Sci. Numer. Simul.*, **89** (2020), 105343. https://doi.org/10.1016/j.cnsns.2020.105343

4. E. Godlewski, P. A. Raviart, *Numerical approximation of hyperbolic systems of conservation laws*, Springer, New York, 1996. https://doi.org/10.1007/978-1-4612-0713-9

5. L. C. Evans, *Partial differential equations*, American Mathematical Society, 1998.

6. R. J. LeVeque, *Finite volume methods for hyperbolic problems*, Cambridge University Press, 2002. https://doi.org/10.1017/CBO9780511791253

7. M. A. E. Abdelrahman, On the shallow water equations, *Z. Naturforschung A*, **72** (2017), 873–879. https://doi.org/10.1515/zna-2017-0146

8. K. Mohamed, M. A. E. Abdelrahman, The modified Rusanov scheme for solving the ultra-relativistic Euler equations, *Eur. J. Mech.-B/Fluids*, **90** (2021), 89–98. https://doi.org/10.1016/j.euromechflu.2021.07.014

9. M. A. E. Abdelrahman, On the shallow water equations, *Z. Naturforschung A*, **72** (2017), 873–879. https://doi.org/10.1515/zna-2017-0146

10. E. F. Toro, *Riemann solvers and numerical methods for fluid dynamics*, Springer Berlin, Heidelberg, 1999. https://doi.org/10.1007/b79761

11. Z. Fu, Z. Tang, Q. Xi, Q. Liu, Y. Gu, F. Wang, Localized collocation schemes and their applications, *Acta Mech. Sin.*, **38** (2022), 422167. https://doi.org/10.1007/s10409-022-22167-x

12. Z. J. Fu, Z. Y. Xie, S. Y. Ji, C. C. Tsai, A. L. Li, Meshless generalized finite difference method for water wave interactions with multiple-bottom-seated-cylinder-array structures, *Ocean Eng.*, **195** (2020), 106736. https://doi.org/10.1016/j.oceaneng.2019.106736

13. A. R. Alharbi, M. B. Almatrafi, New exact and numerical solutions with their stability for Ito integro-differential equation via Riccati–Bernoulli sub-ODE method, *J. Taibah Univ. Sci.*, **14** (2020), 1447–1456. https://doi.org/10.1080/16583655.2020.1827853

14. M. A. E. Abdelrahman, M. B. Almatrafi, A. Alharbi, Fundamental solutions for the coupled KdV system and its stability, *Symmetry*, **12** (2020), 429. https://doi.org/10.3390/sym12030429

15. M. A. E. Abdelrahman, A. Alharbi, Analytical and numerical investigations of the modified Camassa-Holm equation, *Pramana-J. Phys.*, **95** (2021), 117. https://doi.org/10.1007/s12043-021-02153-6

16. K. Mohamed, *Simulation numérique en volume finis, de problémes d'écoulements multidimensionnels raides, par un schéma de flux á deux pas*, Doctoral dissertation, Université Paris-Nord-Paris XIII, 2005.

17. K. Mohamed, M. Seaid, M. Zahri, A finite volume method for scalar conservation laws with stochastic time-space dependent flux function, *J. Comput. Appl. Math.*, **237** (2013), 614–632. https://doi.org/10.1016/j.cam.2012.07.014

18. F. Benkhaldoun, K. Mohamed, M. Seaid, A generalized Rusanov method for Saint-Venant equations with variable horizontal density, In: J. Fořt, J. Fürst, J. Halama, R. Herbin, F. Hubert, *Finite volumes for complex applications VI problems & perspectives*, Springer Proceedings in Mathematics, Springer, Berlin, Heidelberg, **4** (2011), 89–96. https://doi.org/10.1007/978-3-642-20671-9_10
19. K. Mohamed, F. Benkhaldoun, A modified Rusanov scheme for shallow water equations with topography and two phase flows, *Eur. Phys. J. Plus*, **131** (2016), 207. https://doi.org/10.1140/epjp/i2016-16207-3
20. K. Mohamed, H. A. Alkhidhr, M. A. E. Abdelrahman, The NHRS scheme for the Chaplygin gas model in one and two dimensions, *AIMS Math.*, **7** (2022), 17785–17801. https://doi.org/10.3934/math.2022979
21. K. Mohamed, M. A. E. Abdelrahman, The NHRS scheme for the two models of traffic flow, *Comp. Appl. Math.*, **42** (2023), 53. https://doi.org/10.1007/s40314-022-02172-y
22. K. Mohamed, S. Sahmim, M. A. E. Abdelrahman, A Predictor-corrector scheme for simulation of two-phase granular flows over a moved bed with a variable topography, *Eur. J. Mech.-B/Fluids*, **96** (2022), 39–50. https://doi.org/10.1016/j.euromechflu.2022.07.001
23. M. Dumbser, D. S. Balsara, A new efficient formulation of the HLLM Riemann solver for general conservative and non-conservative hyperbolic systems, *J. Comput. Phys.*, **304** (2016), 275–319. https://doi.org/10.1016/j.jcp.2015.10.014
24. R. J. LeVeque, Balancing source terms and flux gradients in high-resolution godynov methods: the quasi-steady wave propagation algorithm, *J. Comput. Phys.*, **146** (1998), 346–365. https://doi.org/10.1006/jcph.1998.6058
25. L. Gosse, A well-balanced scheme using non-conservative products designed for hyperbolic systems of conservation laws with source terms, *Math. Models Methods Appl. Sci.*, **11** (2001), 339–365. https://doi.org/10.1142/S021820250100088X
26. A. Bermudez, M. E. Vazquez, Upwind methods for hyperbolic conservation laws with source term, *Comput. Fluids*, **23** (1994), 1049–1071. https://doi.org/10.1016/0045-7930(94)90004-3

AIMS Press